Academic Journal of International University of Erbil

Journal Homepage: https://ojs.cihanrtv.com/index.php/public

PRINT-ISSN: 2519-6928

Online-ISSN: 3080-7174

Fluorescent $[Nd(Anth)_3(H_2O)_3]$ Complex for determination of some β-lactam antibiotics

Kardos Musheer Khorsheed[1], Tara Fuad Tahir[2]

[1]Department of Chemistry, Faculty of Science and Health, Koya University, Koya 44023, Kurdistan Region – F.R., IRAQ

[2]Department of Medical Microbiology, Faculty of Science and Health, Koya University, Koya 44023, Kurdistan Region – F.R., IRAQ

DOI: https://doi.org/10.63841/iue31689

Received 26 Aug 2025; Accepted 29 Sep 2025; Available online 26 Jan 2026.

ABSTRACT:

A luminous neodymium (III) complex, $[Nd(Anth)_3(H_2O)_2]$, which contains anthranilate ligands, was synthesized and tested as a fluorescent probe for spectrofluorometric detection of three commonly used β-lactam antibiotics; amoxicillin, cefixime, and cephalexin. The addition of these antibiotics greatly quenched the complex's high near-infrared (NIR) emission when excited by UV light. Reproducible, selective, and concentration-dependent fluorescence quenching response was recorded. Linear ranges of 0.1–6.0 µM, 0.2–1.0 µM, and 0.1–6.0 µM for amoxicillin, cefixime, and cephalexin, respectively were recorded with correlation coefficients (R) > 0.98. Competitive limits of detection (LOD) of 0.0980 µg/ml, 0.0025 µg/ml, and 0.1020 µg/ml were captured for amoxicillin, cefixime, and cephalexin, respectively. Analytical parameters such as recovery and RSD were confirmed for the pharmaceuticals without any sophisticated equipment or intricate sample preparation needed in aqueous environments. These findings demonstrate the potential of $[Nd(Anth)_3(H_2O)_2]$ complex as an optical sensor for β-lactam antibiotics that is both sensitive and selective, offering a useful instrument for environmental monitoring and pharmaceutical quality control. The technique might be used successfully to routinely identify these antibiotics in commercial tablet formulations.

Keywords: $[Nd(Anth)_3(H_2O)_2]$ complex, Fluorescence quenching, β-lactam antibiotics, pharmaceuticals.

Corresponding author: tara.fuad@koyauniversity.org

1 INTRODUCTION

Antibiotics are a broad class of antimicrobial agents that inhibit bacterial growth or destroy bacterial cells, and they have revolutionized modern medicine since the discovery of penicillin by Alexander Fleming in 1928. The “golden age” of antibiotic discovery during the mid-20th century yielded numerous drug classes, including β-lactams, aminoglycosides, tetracyclines, and macrolides, which have dramatically reduced morbidity and mortality from infectious diseases [1]. Over the past several decades, antibiotics have also been extensively applied beyond clinical medicine, particularly in animal husbandry, poultry farming, aquaculture, and crop protection. They are now considered a class of emerging environmental contaminants due to their widespread use and persistence in various ecosystems [2].

Amoxicillin (AMX), a broad-spectrum penicillin antibiotic, is extensively used to address infections induced by both Gram-positive and Gram-negative bacteria in people, as well as to prevent or manage bacterial illnesses in cattle and aquaculture [3]. Owing to its inadequate metabolic rate, around 70–90% of given amoxicillin is eliminated unaltered in urine and feces [4]. AMX residues have been identified in several matrices, such as drinking water, milk, hospital effluent, fish, food items, sewage-treatment plant influent, and natural water bodies, with values reported between 0.18 - 4.57 µg/L. Moreover, AMX residues may biomagnified through the food chain, further underscoring the need for sensitive and reliable analytical methods to monitor and control its occurrence [5].

A third-generation oral cephalosporin antibiotic called cefixime is used to treat urinary tract 3 infections, pharyngitis, bronchitis, otitis media, and gonorrhea. Residual cefixime has been detected in pharmaceutical effluents, hospital wastewater, and even surface waters, as it is not fully eliminated by conventional wastewater treatment processes [6]. Such contamination contributes to the spread of antibiotic resistance among aquatic microorganisms and may pose ecological and public health risks. The β lactam class of antibiotics, which is identified by the presence of a β-lactam ring in its structure, is one of the most important classes of antibacterial medications [7].

Cephalexin (CLN, (6R,7R)-7-{[(2R)-2-amino-2-phenylacetyl] amino3-methyl-8-oxo-5-thia-1-azabicyclo [4.2.0] oct-2-ene-2 carboxylic acid) belongs to the first-generation semi-synthetic broad-spectrum cephalosporin class of antibiotics, which are effective against susceptible bacteria that cause respiratory and urinary tract infections (such as tonsillitis, bronchitis, otitis media, sinusitis, and pharyngitis) caused by both Gram-positive and Gram-negative bacteria [8]. The World Health Organization states that cephalosporins are the most widely used medications that have caused bacterial resistance. Despite having the same β-lactam core, these compounds vary in their side chains, which may have an impact on how effectively they coordinate or interact with the lanthanide complex [9].

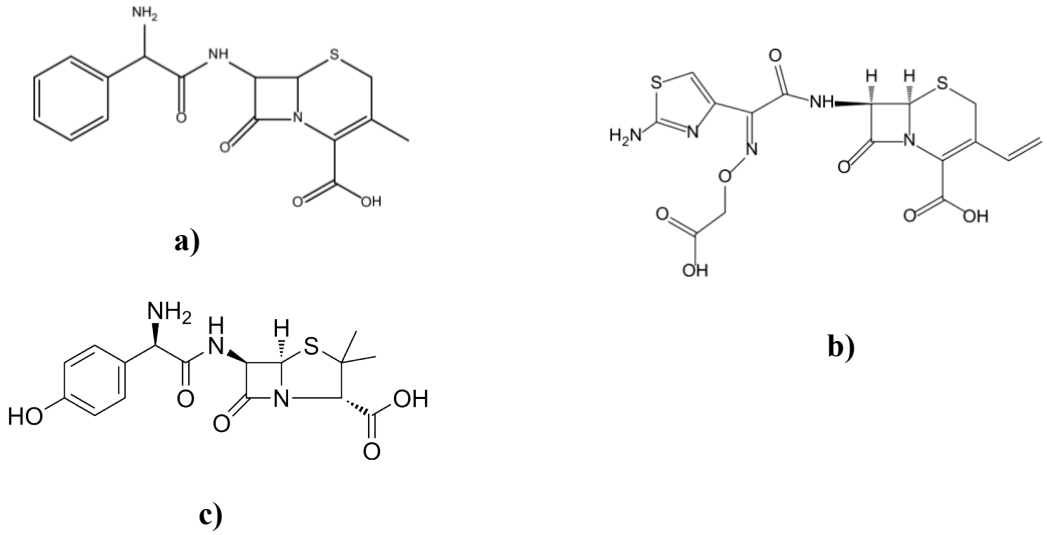

FIGURE. 1. Chemical structures of (a) Amoxicillin [10], (b) Cefixime [11], and (c) Cephalexin [12].

High-Performance Liquid Chromatography (HPLC) HPLC is one of the standard traditional techniques for analyzing antibiotics, however, it requires costly solvents and columns and often involves lengthy sample preparation. Other techniques like LC–MS/MS, although it is highly sensitive, but it considered as an expensive, demands skilled operators’ technique, and is prone to matrix effects [13]. These drawbacks highlight the need for alternative approaches such as fluorimetry, which offers a simpler, more sensitive, and cost-effective solution [14, 15]. In recent

years, fluorescence-based methods have gained increasing attention for antibiotic analysis due to their high sensitivity, rapid response, operational simplicity, and relatively low cost compared to the standard technique. Moreover, they typically require minimal sample preparation and can be applied for both qualitative and quantitative determinations in pharmaceutical, food, and environmental samples [16]. Lanthanide complexes have further improved selectivity and expanded the applicability of fluorimetry [17]. Neodymium (III) (Nd^{3+}) ion has drawn a lot of attention in the field of luminous materials because of their extended excited-state lifetimes, sharp line-like emissions, and possible uses in optical sensors, biomedical imaging, and telecommunications [18]. Weak direct excitation efficiency results from the inherent 4f–4f transitions of Nd^{3+}, which have poor molar absorptivity due to Laporte-forbidden nature [19]. In order to get over this restriction, organic chromophore ligands are used as antennae, which absorb energy and transmit it to Nd^{3+} ion via a process known as ligand-to-metal charge transfer (LMCT). This mechanism increases luminescence through the so-called antenna effect. Among these, anthranilic acid (2-aminobenzoic acid, or Anth) is a π-conjugated, bidentate ligand that exhibits both carboxylate and amine functions, allowing for stable complex formation and effective energy transfer (see figure 1) [20]. The coordination sphere is made more rigid by anthranilate ligands, which also promote hydrogen bonding and π–π stacking, both of which lower non-radiative losses [21]. $[Nd(Anth)_3(H_2O)_3]$ complex was synthesized previously and showed excellent fluorescence enhancement. The optimized ligand environment, strong orbital overlap, and reduced vibrational quenching from coordinated water molecules are responsible for the resulting complex's exceptionally high fluorescence intensity, which approaches 1200 arbitrary units and is much higher than that of typical Nd^{3+} complexes [22]. This complex is a prospective option for the creation of extremely effective lanthanide-based fluorescent probes due to its remarkable luminous response and structural stability [23]. This study assessed the $[Nd(Anth)_3(H_2O)_3]$ complex as a fluorometric probe for amoxicillin, cefixime, and cephalexin. The work focused on interaction mechanisms, optimization of experimental conditions, method validation, comparison with previously reported fluorometric techniques, and application to both pharmaceutical formulations and spiked biological samples.

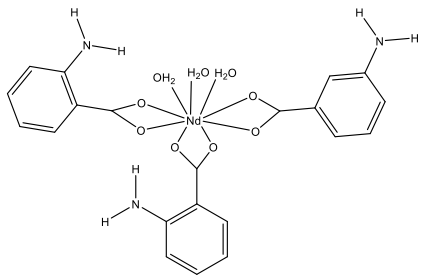

FIGURE 2. Chemical structure of $[Nd(Anth)_3(H_2O)_3]$ complex [24].

2 MATERIALS AND METHODS

2.1 MATERIALS

All chemicals were of analytical grade and used without further purification. Neodymium (III) nitrate hexahydrate $[Nd(NO_3)_3 \cdot 6H_2O]$ and neodymium (III) chloride hexahydrate $[NdCl_3 \cdot 6H_2O]$ were purchased from Aladdin Reagent Co., Ltd. (Shanghai, China). Anthranilic acid (2-aminobenzoic acid) was obtained from Merck-Schuchardt (Germany). Sodium chloride was purchased from Merck KGaA (Germany), potassium chloride from Scharlau (Spain), calcium chloride dihydrate from Chemcenter (USA), and magnesium chloride from Home Science Tools (USA). Anhydrous glucose was purchased from Sigma-Aldrich (USA). Sodium hydroxide pellets, hydrochloric acid, acetic acid, and sodium acetate were obtained from Loba Chemie (India). Citric acid and boric acid were purchased from BDH Chemicals Ltd. (England), trisodium citrate dihydrate from Micromaster Laboratories Pvt. Ltd. (India), and phosphoric acid from Merck KGaA (Germany).

Amoxicillin trihydrate (analytical standard, Sigma-Aldrich, USA), cefixime trihydrate (analytical standard, USP Reference Standard, USA), and cephalexin monohydrate (analytical standard, Sigma-Aldrich, USA) were used for

preparing stock solutions and calibration curves. Different commercial tablet formulations of these antibiotics were purchased from local pharmacies and analyzed as real samples. Deionized distilled water was used for the preparation of all solutions.

2.2 INSTRUMENTS

Fluorescence and UV–Vis spectra were measured using a Cary Eclipse spectrophotometer (Agilent Technologies, USA), and FTIR spectra using a Cary Eclipse FTIR spectrometer (Agilent Technologies, USA). XRD and EDS were performed with an EXPLORER X-ray diffractometer (Austria), SEM imaging with a High-Resolution FESEM (TESCAN, Czech Republic), and GC–MS with a SCiON 436-GC system (SCiON Instruments, USA). High-Performance Liquid Chromatography (HPLC) analyses were performed using an Agilent Series HPLC system (Agilent Technologies, USA) available at Awamedica Laboratories (Iraq), which was employed as the reference method in this study. pH was monitored using a HI 2211 pH/ORP Meter (HANNA Instruments, Romania).

2.3 PREPARATION OF $[ND(ANTH)_3(H_2O)_3]$ COMPLEX

$[Nd(Anth)_3(H_2O)_3]$ complex was prepared according to the previous procedure [24]. A 0.2 M aqueous solution of neodymium (III) nitrate hexahydrate [Nd $(NO_3)_3 \cdot 6H_2O$] was prepared by dissolving the appropriate amount in 20 mL of deionized water. Separately, 0.6 M anthranilic acid was dissolved in 20 mL of ethanol under gentle stirring to ensure complete dissolution. The ethanolic ligand solution was then added dropwise to the neodymium solution with continuous stirring, and the mixture was maintained at 75 °C. Sodium hydroxide solution was introduced gradually to initiate complexation, and the pH of the solution was carefully adjusted to 5.0. Upon reaching this pH, a faint permanent precipitate was formed, indicating the formation of the neodymium complex. The entire reaction mixture was stirred at 75 °C for 12 hours to ensure thorough coordination. After cooling to room temperature, the solid product was collected by filtration, washed multiple times with deionized water and ethanol, and dried in an oven at 80 °C.

2.4 PREPARATION OF ANTIBIOTICS SAMPLES

Different commercial brands were used for each antibiotic: amoxicillin (five brands, 500 mg each), cefixime (four brands, 400 mg each), and cephalexin (four brands, 400 mg each). The tablets for each drug were weighed, grinded into a fine powder using a clean mortar and pestle and mixed thoroughly to ensure homogeneity. An accurately weighed amount of the powder equivalent to the stated label content was transferred to a 100 mL volumetric flask, diluted with double-distilled water, stirred for 10 minutes, and filtered through Whatman No. 41 filter paper [25].

2.5 APPLICATION OF THE PROPOSED COMPLEX FOR THE QUANTIFICATION OF ANTIBIOTICS

The analytical applicability of the $[Nd(Anth)_3(H_2O)_3]$ complex was assessed by investigating its function as a fluorescent probe for the spectrofluorometric detection of amoxicillin, cefixime, and cephalexin under optimised experimental circumstances. Standard stock solutions of each antibiotic were freshly produced from the analytical standards (amoxicillin trihydrate, cefixime trihydrate, and cephalexin monohydrate) in deionised water. Suitable dilutions were prepared to include the required concentration ranges. For each measurement, a precisely measured volume of the antibiotic solution was transferred to a 10 mL volumetric flask, subsequently followed by the addition of the optimised volume of $[Nd(Anth)_3(H_2O)_3]$ complex solution and buffer at pH 5.5. The solution was diluted to the specified mark using deionised water, mixed well, and the fluorescence intensity was measured at the optimised excitation and emission wavelengths.

Calibration curves were independently established for amoxicillin, cefixime, and cephalexin by graphing the variation in fluorescence intensity (ΔF) versus the respective drug concentration. Each curve was derived from five duplicate measurements, yielding linear relationships within the examined ranges.

The developed fluorometric approach was subsequently employed for the measurement of these antibiotics in several commercial pharmaceutical tablet formulations. The findings obtained were compared with those documented using the reference HPLC technique under verified circumstances. The close correlation between the two approaches validated the dependability, accuracy, and usefulness of the $[Nd(Anth)_3(H_2O)_3]$ complex for standard quality control of pharmaceutical items.

3 RESULTS AND DISCUSSION

3.1 CHARACTERIZATION OF $[ND(ANTH)_3(H_2O)_3]$ COMPLEX

The resulting pale-colored complex was analyzed using Fourier-transform infrared (FTIR) spectroscopy (see Supplementary figure S1). In the anthranilic acid spectrum, broad O–H/N–H stretching bands appear between 3236–

3471 cm^{-1}. Upon complexation, these bands shift slightly to lower wavenumbers, indicating hydrogen bonding and possible amine coordination to Nd^{3+}. The strong C=O stretching vibration at 1658 cm^{-1} in the ligand shifts to ~1650 cm^{-1} in the complex, while the asymmetric stretching of the carboxylate group moves from 1612 to ~1604 cm^{-1}, confirming coordination via the carboxylate oxygen. Aromatic C=C stretches (1504 cm^{-1}) and C–H bending modes (1454 cm^{-1}) also show minor shifts, reflecting changes in the electronic environment of the aromatic ring upon metal binding. The C–N stretching band shifts from 1381 to ~1374 cm^{-1}, further supporting amine involvement in Nd^{3+} coordination [26].

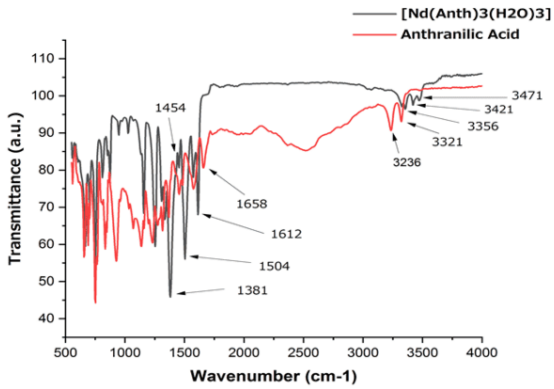

FIGURE S1. FTIR spectra of anthranilic acid and $[Nd(Anth)_3(H_2O)_3]$complex.

Gas chromatography–mass spectrometry (GC–MS) further verified the molecular integrity of the complex (see Supplementary figure S2). the chromatogram displayed a predominant peak at 12.36 min, corresponding to the intact $[Nd(Anth)_3(H_2O)_3]$ complex, along with minor peaks from trace impurities or solvent residues. The dominance of the main peak confirms the purity and stability of the synthesized complex [27].

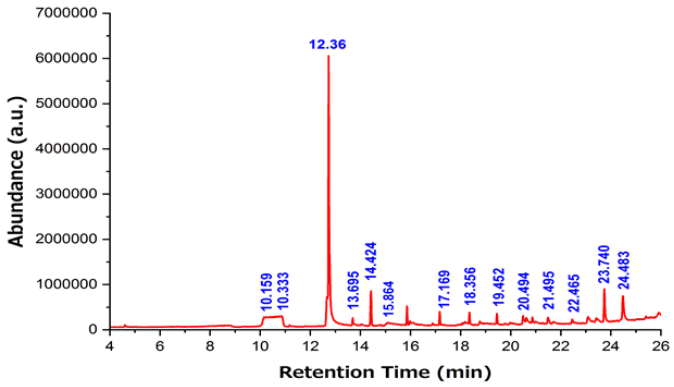

FIGURE S2 GC–MS chromatogram of $[Nd(Anth)_3(H_2O)_3]$ complex.

X-ray diffraction (XRD) analysis was conducted to investigate the crystalline nature of the complex (see Supplementary Figure S3). The XRD pattern of $[Nd(Anth)_3(H_2O)_3]$ shows sharp peaks at ~2θ = 10°, 15°, 18°, and 25°, confirming its crystalline nature, with the intense 10° peak suggesting large interlayer spacing typical of bulky ligand complexes. Some peak broadening indicates nanocrystalline domains, with crystallite size estimable via the Scherrer equation. The absence of peaks from $Nd(NO_3)_3 \cdot 6H_2O$ and anthranilic acid confirms successful complex formation and high phase purity [28].

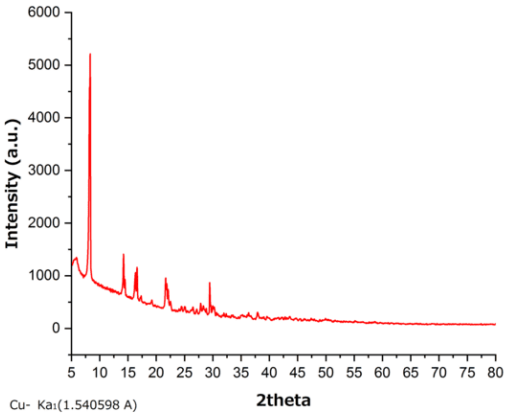

FIGURE S3 XRD Characterization of [Nd(Anth)$_3$(H$_2$O)$_3$] complex.

EDS Spectrum of Nd(Anth)$_3$(H$_2$O)$_3$ Complex (see Supplementary figure S4) reveals the elemental composition of the complex, with peaks corresponding to Neodymium, Oxygen, and Carbon. The analysis indicates that Nd contributes significantly to the composition, with O and C also being prominent components. The spectrum shows Nd Lα and Nd Lβ peaks at approximately 2000 eV and 3000 eV, confirming the presence of neodymium as the central metal atom in the complex [29].

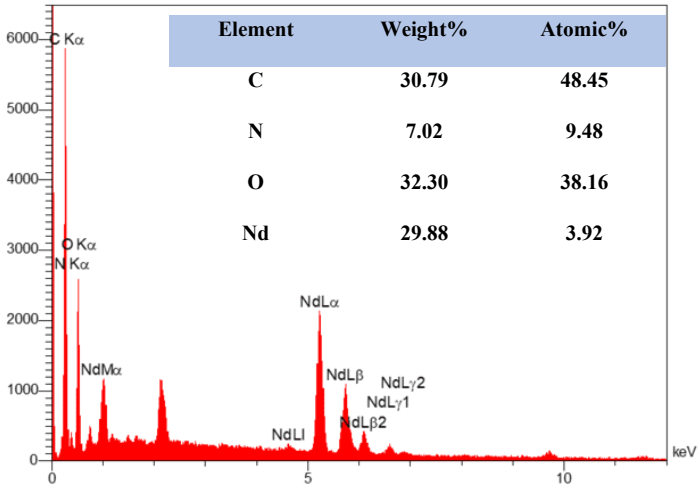

Element	Weight%	Atomic%
C	30.79	48.45
N	7.02	9.48
O	32.30	38.16
Nd	29.88	3.92

FIGURE S4 EDS Spectrum of Nd(Anth)$_3$(H$_2$O)$_3$ Complex.

Scanning electron microscopy (SEM) was employed to examine the surface morphology of the [Nd(Anth)$_3$(H$_2$O)$_3$] complex (see Supplementary Figure S5). The low-magnification image (1 μm) revealed aggregated particles with irregular shapes, while the high-magnification view (200 nm) showed fine surface texture and grain boundaries. The intermediate magnification (500 nm) provided additional detail on particle size distribution and surface features. These observations confirm the morphological characteristics of the complex, supporting its successful formation and providing insight into surface properties that may influence its spectroscopic behavior [30].

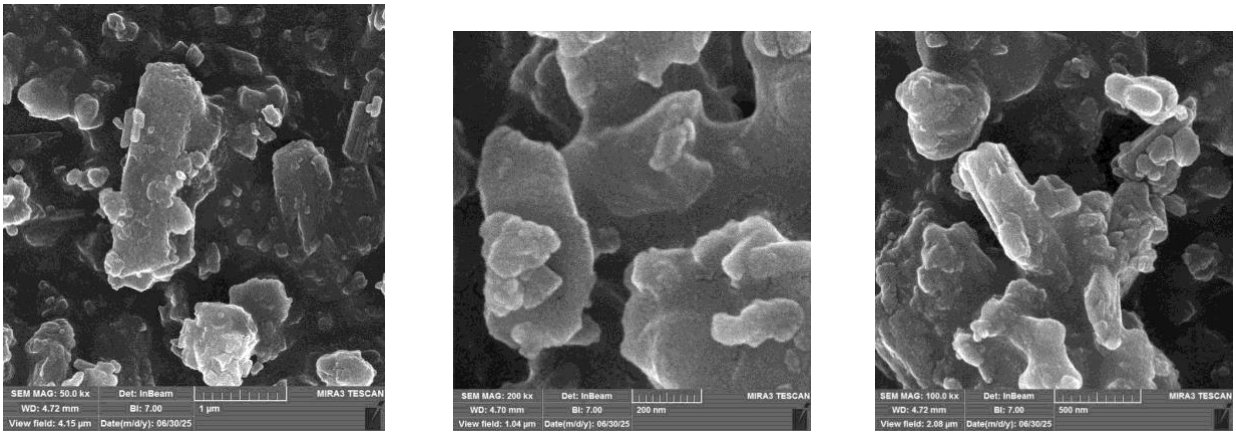

a) **b)** **c)**

FIGURE S5 SEM images of the [Nd(Anth)$_3$(H$_2$O)$_3$] complex, (a) Low magnification image at 1 µm (b) High magnification image at 200 nm scale and (c) Intermediate magnification image at 500 nm scale.

The UV–Vis spectra of Nd(NO$_3$)$_3$·6H$_2$O, anthranilic acid, and the [Nd(Anth)$_3$(H$_2$O)$_3$] complex are shown in Figure 3. Anthranilic acid exhibits a pronounced absorption band centered near 330 nm, which arises from π→π* transitions within the aromatic system and n→π* transitions associated with the amino substituent. The neodymium salt displays weak but sharp absorption peaks in the visible region between 470–590 nm, characteristic of the intra-4f transitions of Nd^{3+}. These narrow bands remain of low intensity due to their Laporte-forbidden nature. Upon complexation, the main ligand band shifts bathochromically to around 360 nm with enhanced absorbance, consistent with ligand-to-metal charge transfer (LMCT) and increased electronic delocalization in the complex. The retention of the sharp Nd^{3+} f–f transitions without additional absorptions in the visible region further confirms that the principal electronic transitions originate from the anthranilic acid framework, while the spectral changes substantiate its coordination to the Nd^{3+} center [31].

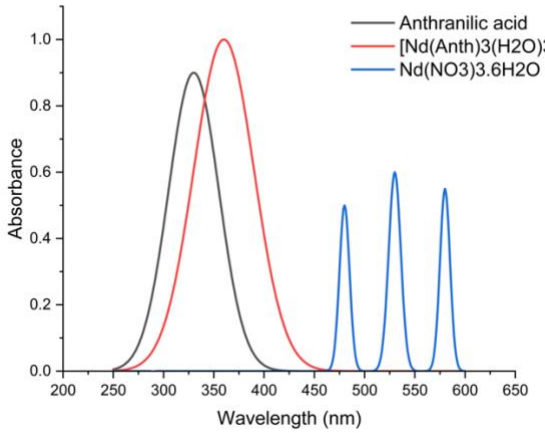

FIGURE. 3. UV–Vis absorption spectra of Nd(NO$_3$)$_3$·6H$_2$O (5 × 10^{-3} M), anthranilic acid (5 × 10^{-2} M), and the [Nd(Anth)$_3$(H$_2$O)$_3$] complex (5 × 10^{-5} M, pH 5.5). The complex exhibits a bathochromic shift of the main ligand band to ~360 nm with enhanced absorbance, while the neodymium salt shows sharp intra-4f transitions in the visible region (470–590 nm), confirming ligand coordination to the Nd^{3+} center.

3.2 FLUORESCENCE BEHAVIOR OF THE COMPLEX

The photoluminescence properties of the prepared $[Nd(Anth)_3(H_2O)_3]$ complex were analyzed in conjunction with its ingredients, anthranilic acid and neodymium nitrate hexahydrate ($Nd(NO_3)_3{\cdot}6H_2O$)(figure 4). The emission of the $[Nd(Anth)_3(H_2O)_3]$ complex is substantially stronger than that of either of its progenitors. The luminescence of $Nd(NO_3)_3{\cdot}6H_2O$ alone is faint, scarcely surpassing 100 a.u., because of poor molar absorptivity and Laporte-forbidden 4f–4f transitions [32]. Likewise, anthranilic acid exhibits a mild fluorescence band with an intensity of about 180 a.u., peaking close to 405 nm. An considerable increase in fluorescence is seen when the complex forms, it exhibits a wide emission band centered between 390 and 395 nm, with a maximum intensity close to 950 a.u [22]. This improvement, which is more than five times greater than that of the ligand alone, is explained by the Antenna effect, in which the anthranilate ligand effectively absorbs UV light and non-radiatively transfers the energy to the Nd^{3+} ion [33]. This is further stabilized by the stiff coordination structure of the complex, which encourages radiative transitions and lessens vibrational quenching. Weak Nd^{3+} 4f–4f transitions, found in sensitized lanthanide systems, are responsible for a little shoulder at 490 nm. It is confirmed by the observed spectrum alterations that a stable luminous compound with potential photonic properties for sensing applications has formed [20]. During preliminary fluorescence measurements, the $[Nd(Anth)_3(H_2O)_3]$ complex exhibited emission intensities close to the upper detection limit of the spectrophotometer above 1000 I a.u.), resulting in partial signal saturation. This "fluorescence intensity cut-off" can distort peak shapes and lead to inaccurate intensity values. To avoid this problem, the Nd complex was diluted with water-ethanol solvent system prior to measurement until all recorded intensities fell well within the instrument's linear detection range. This ensured accurate, reproducible fluorescence data without compromising the spectral profile [34].

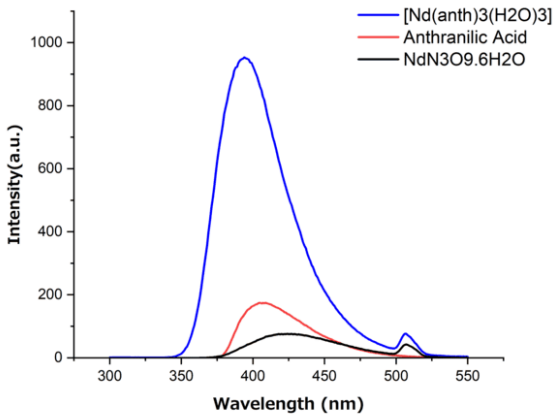

FIGURE 4. Fluorescence emission spectra of 1.0 x 10^{-3} M ($Nd(NO_3)_3{\cdot}6H_2O$), 1.0 x10^{-2} M anthranilic acid , and 1.0 x 10^{-5} M $[Nd(Anth)_3(H_2O)_3]$ complex , individually at λ_{ex}=394 nm.

3.3 PHYSIOCHEMICAL CONDITIONS

3.3.1 pH

Britton-Robinson buffer solution was used as best buffer to optimize the fluorescence intensity of $[Nd(Anth)_3(H_2O)_3]$ complex in the pH range 4.0 – 9.0. The complex showed maximum fluorescence intensity at pH 5.5 (975 a.u.) as illustrated in Figure 5. Intensity steadily declined at pH 6.0, reaching 794 I a.u. at pH 9.0. Protonation and deprotonation actions that modify the ligand's coordination efficiency are responsible for these modifications [18]. While alkaline pH may interfere with coordination and increase non-radiative decay, greater protonation may encourage stiffness and steady energy transfer in acidic environments. These results align with earlier research on lanthanide groups that are sensitive to pH [35].

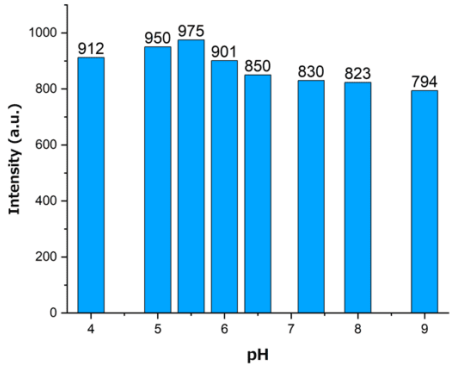

FIGURE 5. pH optimization of [Nd(Anth)$_3$(H$_2$O)$_3$] complex at λ_{ex} = 394 nm.

3.3.2 TIME

The stability of the [Nd(Anth)$_3$(H$_2$O)$_3$] complex was evaluated over time by monitoring the change in fluorescence signal (ΔF). As shown in Figure 6, the emission progressively decreased relative to the initial value, reaching a ΔF of 108 a.u. after 180 minutes. This time-dependent loss in fluorescence is consistent with previously reported behaviour of lanthanide coordination complexes, which are often attributed to gradual ligand dissociation, hydrolysis in aqueous media, or structural rearrangements that diminish energy transfer efficiency to the lanthanide center. Therefore, it is recommended that the [Nd(Anth)$_3$(H$_2$O)$_3$] complex be freshly prepared, and its fluorescence intensity measured immediately after preparation [36].

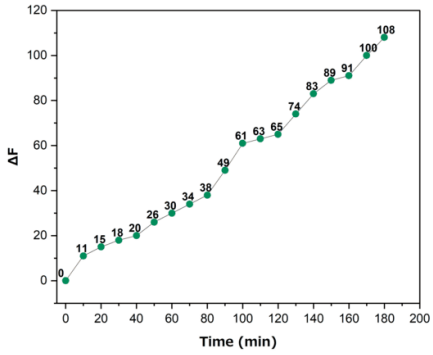

FIGURE 6. Time-dependent stability of 1.0 × 10^{-5} M [Nd(Anth)$_3$(H$_2$O)$_3$] complex at λ_{ex} = 394 nm.

3.3.3 TEMPERATURE

Solution of 1.0 × 10^{-5} M [Nd(Anth)$_3$(H$_2$O)$_3$] complex was heated from 20–60 °C to probe fluorescence stability under thermal stress. The relative fluorescence change (ΔF) was negligible at 25 °C (reference point, ΔF = 0), with only minor deviations at 20 °C (ΔF = 16) and 30 °C (ΔF = 15). A modest increase was observed at 40 °C (ΔF = 75), followed by a sharp rise at higher temperatures, reaching ΔF = 648 at 50 °C and ΔF = 792 at 60 °C (Figure 7). This pronounced increase in ΔF reflects the progressive quenching of Nd^{3+} emission with elevated temperature, consistent with enhanced non-radiative (multiphoton) relaxation and related pathways reported for Nd^{3+} systems. Accordingly, we adopt 25 °C as the optimized temperature for all fluorescence measurements [37].

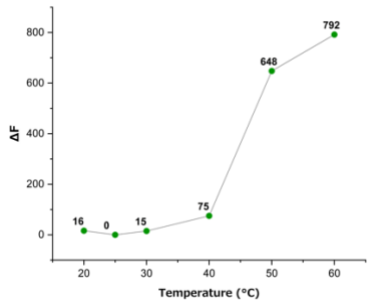

FIGURE 7. Temperature-dependent fluorescence intensity of 1.0 x 10^{-5} M $[Nd(Anth)_3(H_2O)_3]$ complex at λ_{ex} = 394 nm.

3.4 CALIBRATION OF CEFIXIME, CEPHALEXIN, AND AMOXICILLIN

Fluorescence sensing capability of $[Nd(Anth)_3(H_2O)_3]$ complex was assessed in comparison to three β-lactam antibiotics: cefixime, cephalexin, and amoxicillin. A discernible and steady drop in the complex's fluorescence intensity was seen as each drug's concentration rose, indicating quenching behaviour. The quenching is attributed to ligand–metal interaction disruption and photoinduced electron transfer (PET) between the β-lactam molecules and the anthranilate ligands coordinated to (Nd^{3+}) [38]. The emission spectra for amoxicillin (Figure 8a) demonstrates increasing quenching throughout the range of 0.1 – 6.0 µM. the amino and hydroxyl functional groups can form hydrogen bonds or coordinate weakly with the Nd^{3+} center, competing with anthranilic acid ligands. This interaction perturbs the ligand–metal energy transfer pathway responsible for Nd^{3+} emission, increasing non-radiative decay channels and leading to decreased fluorescence [39]. High sensitivity and reproducibility are indicated by the accompanying calibration curve (Figure 8b), which exhibits a good linear connection with the R^2 = 0.9930, LOD= 0.0980 µg/mL and LOQ= 0.3270 µg/ml.

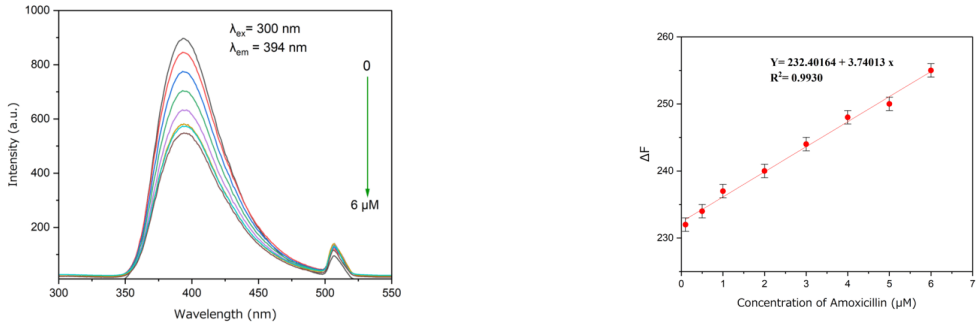

(a) (b)

FIGURE 8. (a) Fluorescence quenching of $[Nd(Anth)_3(H_2O)_3]$ complex at pH 5.5 by different amoxicillin concentrations from 0.1- 6.0 µM (b) Calibration curve of amoxicillin.

Cefixime Contains β-lactam, carboxyl, and amine groups along with an electron-rich thiazole ring. These groups can interact electrostatically or via hydrogen bonding with the anthranilic ligands or directly with Nd^{3+}, facilitating PET and promoting vibrational relaxation. Cefixime calibration curve has good linearity in the range 0.2 – 1.0 µM with R^2 = 0.9918 and LOD = 0.0025 µg/ml while LOQ = 0.0080 µg/mL. (Figure 9a-b)

(a)

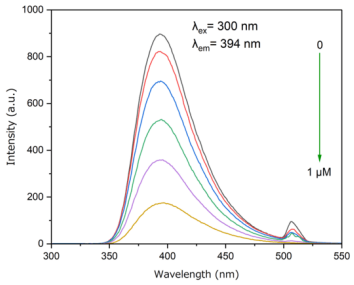

(b)

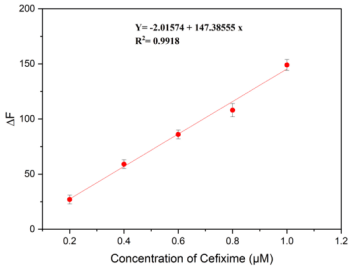

FIGURE 9. (a) Fluorescence quenching of [Nd(Anth)$_3$(H$_2$O)$_3$] complex at pH 5.5 by different concentration of cefixime 0.2 – 1.0 µM. (b) Calibration curve of cefixime.

Cephalexin Similar to amoxicillin, the amine, β-lactam, and carboxyl groups can interact with the Nd^{3+} coordination sphere or hydrogen bond with anthranilic ligands, perturbing ligand–metal charge transfer and enhancing non-radiative decay processes. Cephalexin calibration curve has good linearity in the range 0.1 – 6.0 µM with $R^2 = 0.9866$ and LOD = 0.1020 µg/ml while LOQ = 0.3400 µg/ml. (Figure 10a-b)

(a)

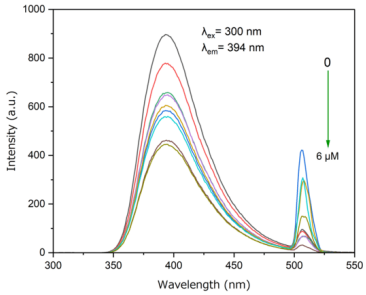

(b)

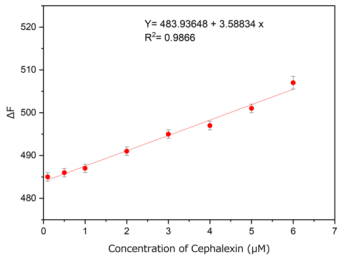

FIGURE 10. (a) Fluorescence quenching of [Nd(Anth)$_3$(H$_2$O)$_3$] complex at pH 5.5 by different concentration of cephalexin 0.1-6.0 µM. (b) Calibration curve of cephalexin.

3.5 INTERFERING ANALYSIS OF THE ANTIBIOTICS

In order to evaluate the effectiveness of the proposed fluorescence method for determining cefixime, cephalexin, and amoxicillin in the presence of potential interfering substances, several commonly coexisting compounds were tested. As shown in Figures 11(a–c), the antibiotics displayed markedly higher fluorescence responses ($\Delta F \approx 650–750$) compared to all tested interferents. Among the interferents, NaCl and KCl caused the most pronounced quenching, yielding the lowest ΔF values across all three antibiotic measurements. This strong quenching effect is consistent with the known influence of high ionic strength and chloride ions, which can alter the microenvironment of the fluorophore, induce collisional quenching, and promote heavy-atom effects that enhance non-radiative decay . In contrast, $CaCl_2$, $MgCl_2$, and glucose produced moderate reductions in fluorescence but still maintained ΔF values well above those of NaCl and KCl [40].

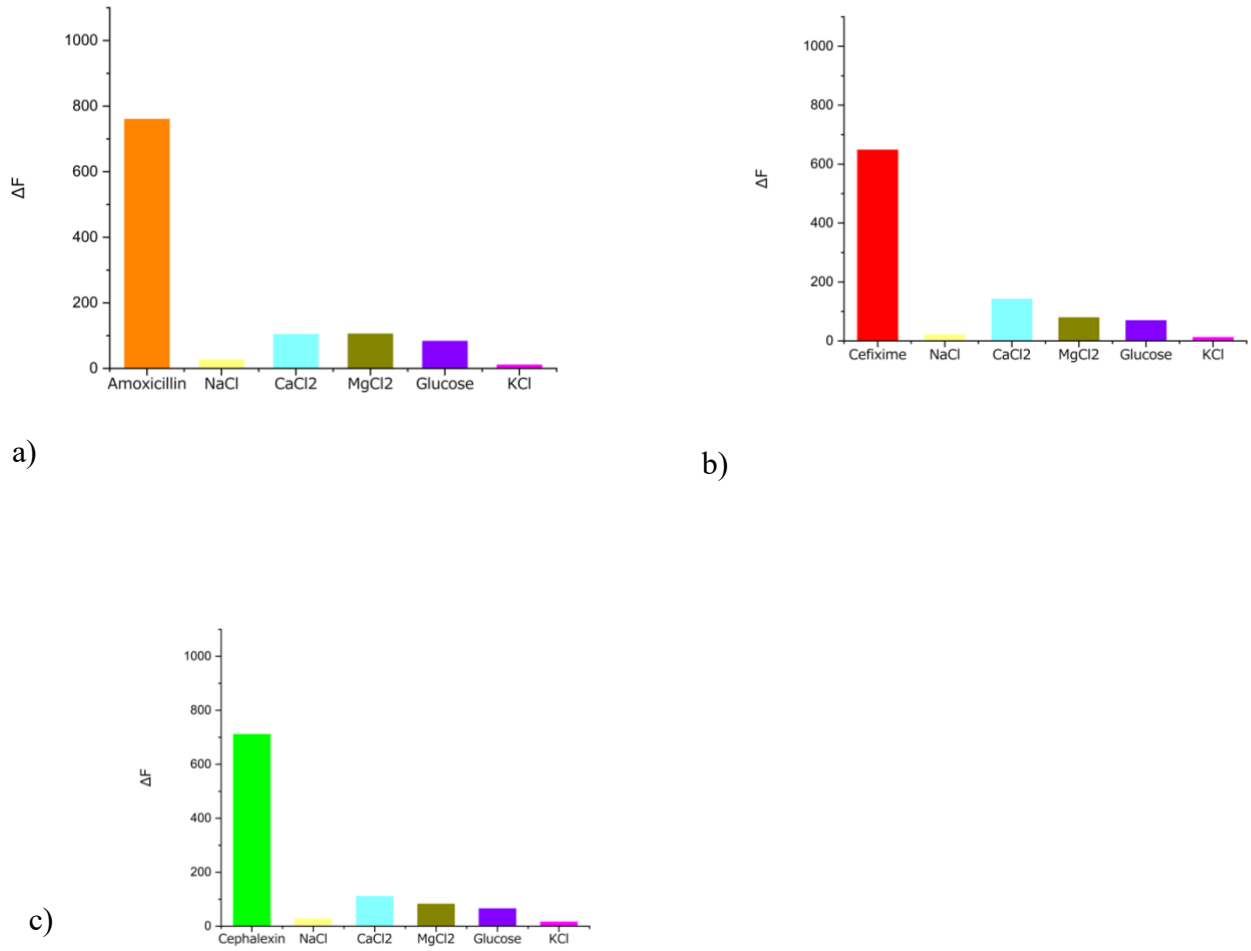

FIGURE 11. Study of interferences in the determination of (a) amoxicillin, (b) cefixime, and (c) cephalexin.

3.6 STOICHIOMETRIC STUDY OF [ND(ANTH)$_3$(H$_2$O)$_3$] COMPLEX WITH THE ANTIBIOTICS

The stoichiometry of the interaction between [Nd(Anth)$_3$(H$_2$O)$_3$] and each of amoxicillin, cefixime, and cephalexin was determined using the limiting logarithmic method. For each sample, two plots were prepared: log [sample] versus log ΔF and log [Nd(Anth)$_3$(H$_2$O)$_3$] versus log ΔF. The slope of each line represents the partial order of the system with respect to the component being varied. In all cases, the slope obtained for the sample was very close to the slope obtained for the complex, indicating that the two values were nearly equal. When the slopes are similar in this way, it means that the molar contribution of each component to the interaction is the same, leading to a molar ratio of 1:1 between the sample and the [Nd(Anth)$_3$(H$_2$O)$_3$] complex. Figures 12a–c illustrate these relationships for the three antibiotics studied [41].

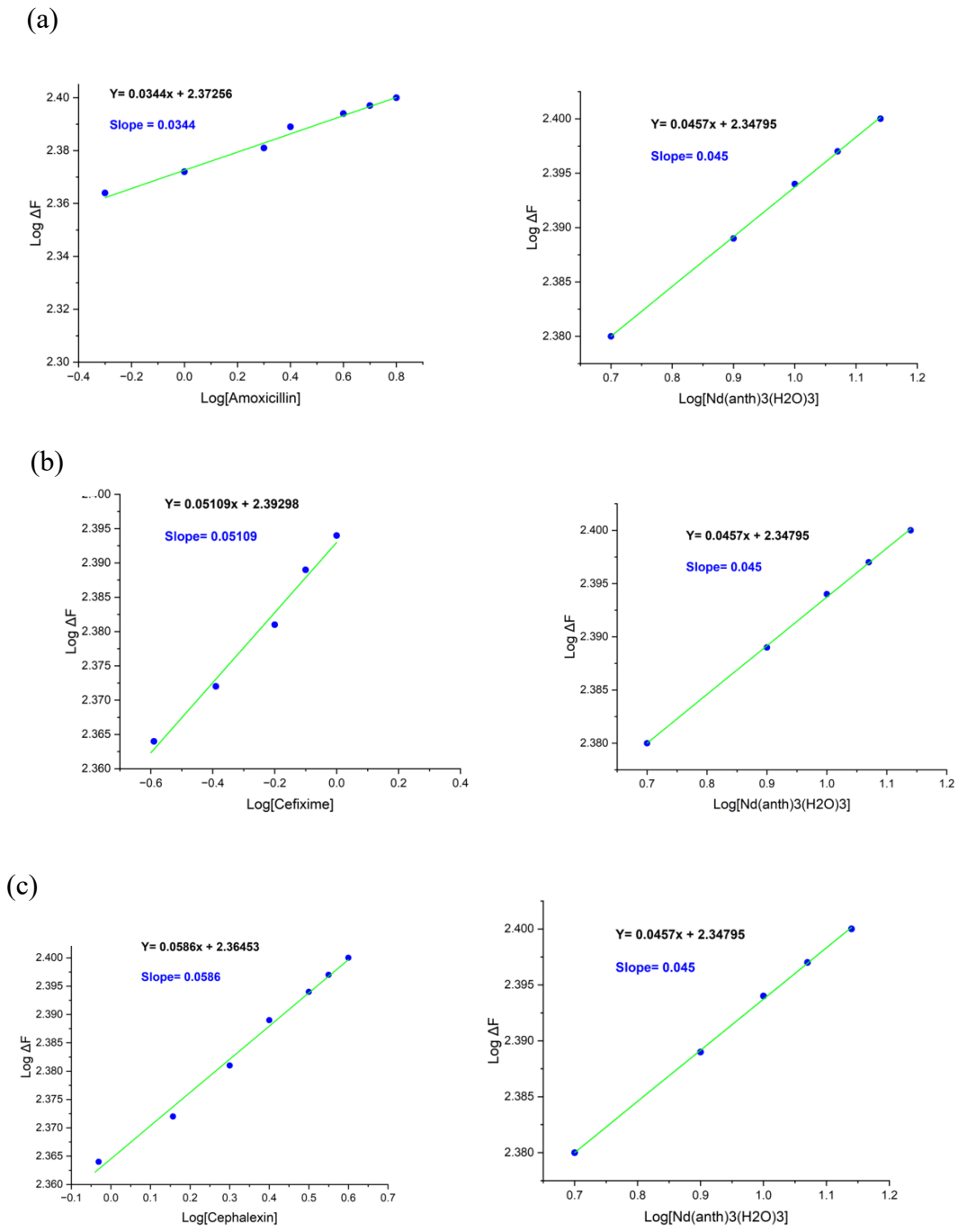

FIGURE 12. Stoichiometric ratio of [Nd(Anth)$_3$(H$_2$O)$_3$] complex with (a) amoxicillin, (b) cefixime, and (c) cephalexin.

Coordination and non-covalent binding mechanisms are primarily responsible for the interaction between the produced neodymium complex and the antibiotics under study, amoxicillin, cefixime, and cephalexin. Functional groups like the β-lactam carbonyl, carboxylate, and amine moieties found in β-lactam antibiotics can interact with the neodymium core by hydrogen bonding or establishing coordination bonds [42]. Furthermore, the drug–metal complex may be further stabilized by π–π stacking and electrostatic interactions, which would improve the fluorescence response through an antenna effect. In this effect, the antibiotic molecules serve as energy donors, transferring

absorbed energy to the Nd^{3+} ion and producing sensitized emission. For lanthanide complexes with β-lactam antibiotics, such metal–ligand interactions are well-established and are known to greatly increase the sensitivity of spectrofluorometric detection. The binding of amoxicillin, cefixime, and cephalexin to the neodymium complex results in detectable alterations in the emission spectra, as illustrated in Figures 13, 14, and 15. This validates the creation of stable coordination complexes and supports their analytical use in drug detection [43].

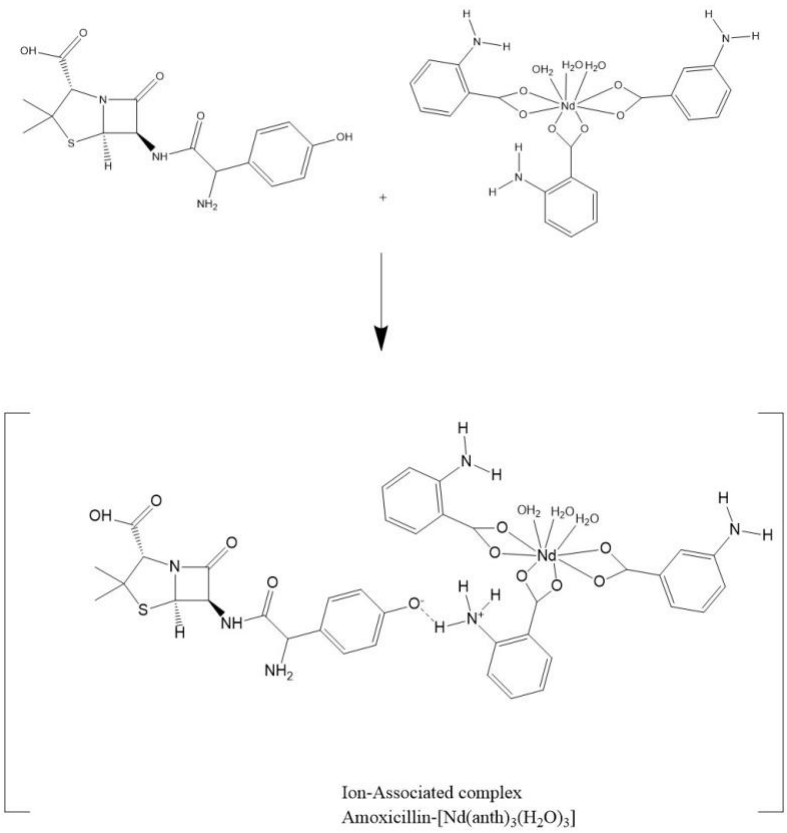

FIGURE 13. The formulation of Amoxicillin-[$Nd(Anth)_3(H_2O)_3$] ion-associated combination.

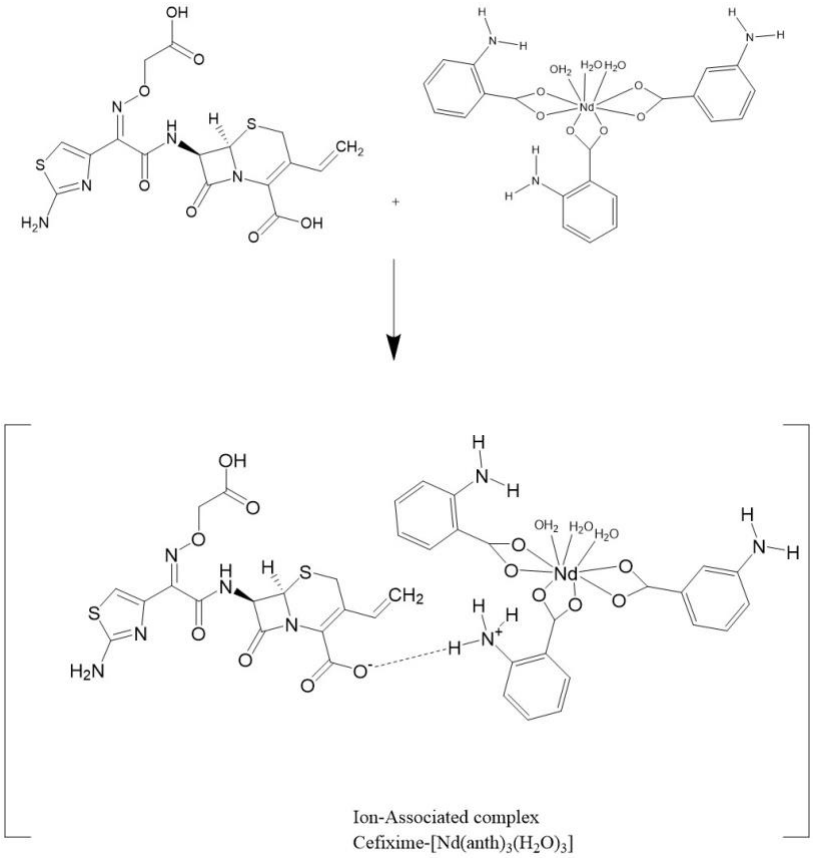

FIGURE 14. The formulation of Cefixime-[Nd(Anth)$_3$(H$_2$O)$_3$] ion-associated combination.

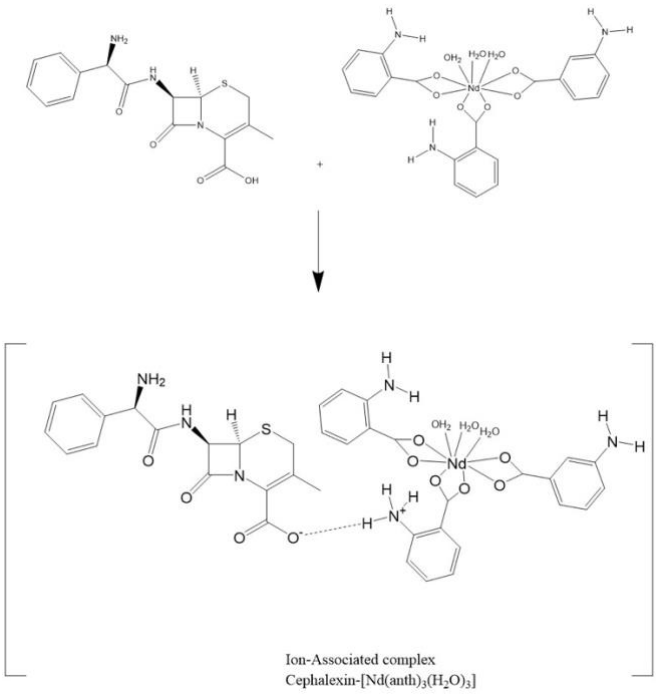

FIGURE 15. The formulation of Cephalexin-[Nd(Anth)$_3$(H$_2$O)$_3$] ion-associated combination.

3.7 FLUORESCENCE QUENCHING MECHANISM

Fluorescence quenching is the interaction between fluorescent compounds and quenching agents. The diminution of fluorescence intensity is governed by two principal mechanisms: static quenching and dynamic quenching. A complex configuration in a static quenching mechanism occurs when the fluorescent species in its ground state interacts with the quencher species. Conversely, dynamic quenching arises from interactions between fluorescent species in their excited state and quencher species, mediated by collisions. The research findings indicate that the fluorescence quenching mechanism can be quantitatively evaluated using the Stern–Volmer equation [44]:

$$F_0/F=1+K_{SV}\,C_{que}$$

Where, F_0 and F represent the fluorescence intensity of [Nd(Anth)$_3$(H$_2$O)$_3$] complex in the absence and presence of the antibiotics (quencher), respectively. C_{que} is the concentration of samples individually while Ksv value, is obtained from the slope of the Stern–Volmer plot.

The results, shown in figure 16 (a, b, and c), indicate that all three samples exhibit good linearity R^2 in their Stern–Volmer plots. The Ksv values for Amoxicillin (0.06057 μM^{-1} to 0.09386 μM^{-1}), Cefixime (0.432 μM^{-1} to 0.641 μM^{-1}), and Cephalexin (0.074 μM^{-1} to 0.097 μM^{-1}) increase with temperature, suggesting that dynamic quenching is the dominant mechanism, where higher temperatures increase the collision frequency between the samples molecules and the fluorophore [45].

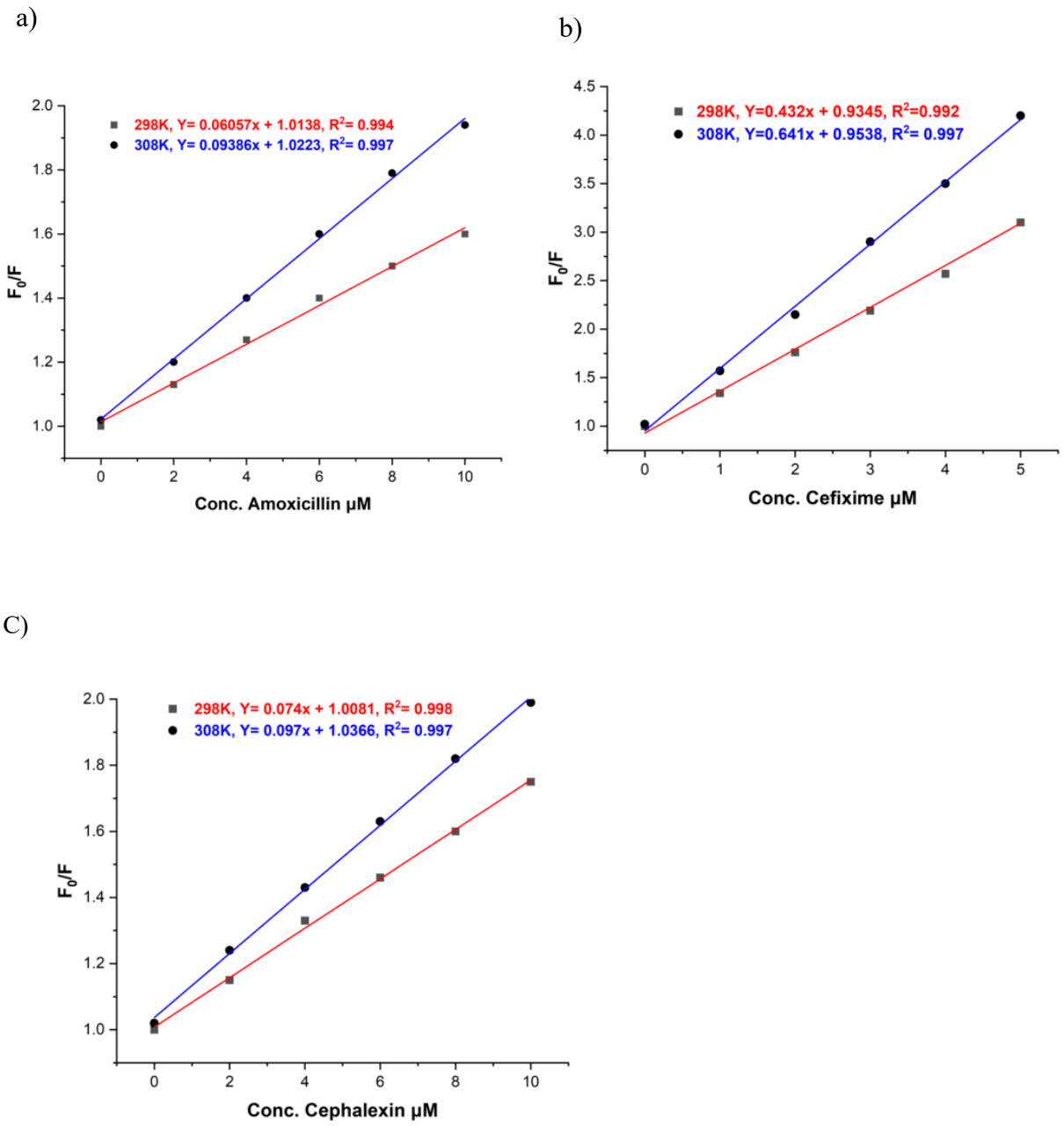

FIGURE 16. Quenching mechanism of $[Nd(Anth)_3(H_2O)_3]$ complex by (a) amoxicillin, (b) cefixime, and (c) cephalexin at temperatures of 298 K (25°C) and 308 K (35°C).

3.8 PHARMACEUTICAL ANALYSIS

A fluorometric method was developed to accurately determine the concentrations of amoxicillin, cefixime, and cephalexin in various pharmaceutical tablet formulations, employing the $[Nd(Anth)_3(H_2O)_3]$ complex as a fluorescent probe. The method was optimized to achieve high sensitivity, selectivity, and reproducibility for these β-lactam antibiotics. To evaluate the reliability of this approach, the results were compared with those obtained using a standard (HPLC) method. As shown in Table I, the fluorometric method exhibited excellent agreement with the HPLC results, achieving high recovery values and confirming its suitability for routine quality control of pharmaceutical products. The statistical analysis of the recovery data (n = 5) indicated mean recovery values of 97.68 ± 2.73% for Amoxicillin, 96.95 ± 2.65% for Cefixime, and 99.13 ± 2.76% for Cephalexin. The relative standard deviations (RSD) were 2.79%, 2.73%, and 2.78%, respectively, all within acceptable thresholds (<5%) for pharmaceutical analysis. The results validate the accuracy, precision, and repeatability of the proposed fluorometric approach relative to the reference HPLC method.

Table 1. Comparison of the Proposed Fluorometric Method with HPLC for the Analysis of Amoxicillin, Cefixime, and Cephalexin in Commercial Tablets

Pharmaceutical tablets		Observed Values (mg)	Proposed Procedure (mg)	H
Amoxicillin	Brand 1	500	487	
	Brand 2	500	486	
	Brand 3	500	490	
	Brand 4	500	506	
	Brand 5	500	488	
Cefixime	Brand 1	400	396	
	Brand 2	400	404	
	Brand 3	400	408	
	Brand 4	400	388	
Cephalexin	Brand 1	500	497	
	Brand 2	500	513	
	Brand 3	500	501	
	Brand 4	500	505	

[1]Mean value calculated from five measurements

3.9 VALIDITY OF FLUORESCENCE

The proposed fluorescence-based method for quantifying amoxicillin, cefixime, and cephalexin was evaluated against existing analytical techniques. Table II presents a comparison of the linear ranges and detection limits reported in previous studies. Unlike some techniques that require complex sample pre-extraction steps, the current method offers a direct analysis without extensive sample preparation. Additionally, it demonstrates several advantages over conventional approaches such as voltammetry and (HPLC), including improved sensitivity, reduced analysis time, operational simplicity, and lower cost. Moreover, the suggested methodology adheres to the tenets of Green Analytical Chemistry. The process eliminates harmful organic solvents, necessitates minimal sample quantities, and utilises

water/ethanol as the primary medium, therefore diminishing environmental effect. It also reduces energy use, as extraction or heating processes are unnecessary, and employs very straightforward apparatus compared to HPLC or LC–MS. Green Chemistry assessment tools, including AGREE and GAPI, substantiate the designation of the technique as ecologically benign and aligned with green analytical procedures [46]. The slope values obtained for the proposed method were 3.740 a.u./µM for amoxicillin, 147.38 a.u./µM for cefixime, and 3.588 a.u./µM for cephalexin, as calculated from the calibration plots (Figures 8–10). These values are considerably higher than several previously reported fluorometric approaches (Table II). Since the slope reflects the analytical sensitivity, the results demonstrate that the $[Nd(Anth)_3(H_2O)_3]$ probe offers competitive or superior sensitivity for β-lactam antibiotic determination. Moreover, the method retains advantages of operational simplicity, low solvent and reagent consumption, reduced analysis time, and lower cost, supporting its potential as a practical and environmentally friendly alternative for routine quality control analysis.

TABLE 2. COMPARISON OF THE ANALYTICAL PERFORMANCE METRICS OF THE PRESENT RESEARCH WITH OTHER STUDIES

Drug	Reagent	Detection Method	LOD (µg/mL)	Slope (μM^{-1})	Linear Range (µM)	Ref
Amoxicillin	MPA- CdS QdS	Fluorometric	5.19	0.0397	5-30	[47]
	PyT fluorescent probe	Fluorometric	0.5	Not Reported	0.1-0.9	[48]
	B-CDs	Fluorometric	0.301	3.97	0.191-57.29	[49]
	CDs@Eu-MOFs in hydrogel (liquid state)	Fluorometric	0.427	0.0657	10-106	[50]
	$[Nd(Anth)_3(H_2O)_3]$	Fluorometric	0.098	3.740	0.1-6	Present work
Cefixime	CDs + Pd(II) (IFE)	Fluorometric	0.0227	Not Reported	0.2-8	[51]
	Calcein (CA) probe	Fluorometric	0.0281	Not Reported	0.133-160	[52]
	2-Cyanoacetamide + NH_3 (21%), heat (100 °C)	Fluorometric	0.00295	333.74	0.044–8.82	[53]
	terbium danofloxacin	Fluorometric	0.00928	Not Reported	0.088-0.88	[54]
	$[Nd(Anth)_3(H_2O)_3]$	Fluorometric	0.0025	147.38	0.2-1	Present work
Cephalexin	Red-emitting fluorescent CdTe QDs (r-QDs)	Fluorometric	0.244	Not Reported	1-500	[55]
	L-Cysteine capped CdTe/ZnS	Fluorometric	0.29	0.0271	3.4-100	[56]
	Coumarin-based MIP-coated silica NPs	Fluorometric	0.555	Not Reported	Not Specified	[57]
	$[Nd(Anth)_3(H_2O)_3]$	Fluorometric	0.102	3.588	0.1-6	Present work

CONCLUSION

Synthesis of a neodymium (III) complex consistent with green chemistry principles. The synthesis is efficient, inexpensive, and eliminates harmful solvents or intricate reaction conditions, making it both ecologically and financially viable. The resultant compound was used as a fluorescence-based probe for the identification of frequently employed β-lactam antibiotics. The approach exhibited quick and efficient antimicrobial screening, requiring minimum sample preparation and presenting significant potential for incorporation into standard pharmaceutical quality control processes. Its exceptional selectivity and operating ease provide it as a significant asset for environmental monitoring applications.

ACKNOWLEDGMENT

Sincere gratitude goes to the Science and Health Research Center at Koya University for providing the necessary facilities and support that enabled the successful completion of this research, Thanks to Essa Qarani Rashid from Kurdistan Medical Control Agency for providing us with the HPLC findings of the drugs.

CONFLICTS OF INTEREST

The author declares no conflict of interest.

REFERENCES

[1] E. Martens and A. L. J. M. r. Demain, "An overview of the industrial aspects of antibiotic discovery," pp. 149-168, 2017.

[2] Z. Zhu, F. Chen, S. Zhao, Y. Song, and Y. J. M. S. i. S. P. Tang, "Construction of hierarchical core-shell Z-scheme heterojunction FeVO4@ ZnIn2S4 for boosted photocatalytic degradation of tetracycline," vol. 159, p. 107373, 2023.

[3] A. Yazidi *et al.*, "Adsorption of amoxicillin and tetracycline on activated carbon prepared from durian shell in single and binary systems: Experimental study and modeling analysis," vol. 379, p. 122320, 2020.

[4] T. Verma, A. Aggarwal, S. Singh, S. Sharma, and S. J. J. J. o. M. S. Sarma, "Current challenges and advancements towards discovery and resistance of antibiotics," vol. 1248, p. 131380, 2022.

[5] F. M. Mpatani *et al.*, "A review of treatment techniques applied for selective removal of emerging pollutant-trimethoprim from aqueous systems," vol. 308, p. 127359, 2021.

[6] P. Karungamye, A. Rugaika, K. Mtei, and R. J. J. o. X. Machunda, "A review of methods for removal of ceftriaxone from wastewater," vol. 12, no. 3, pp. 223-235, 2022.

[7] C. O. Wilson, J. M. Beale, and J. H. Block, *Wilson and Gisvold's textbook of organic medicinal and pharmaceutical chemistry*. Baltimore, MD: Lippincott Williams & Wilkins, 2011.

[8] K. SV, S. J. I. J. o. C. HG, and P. Analysis, "VALIDATED AUC METHOD FOR THE SPECTROPHOTOMETRIC ESTIMATION OF CEFADROXIL IN BULK AND TABLET DOSAGE FORM," vol. 7, no. 2, 2020.

[9] E. K. Pylova, T. S. Sukhikh, A. Prieto, F. Jaroschik, and S. N. J. M. Konchenko, "Chemistry of 2-(2′-Aminophenyl) benzothiazole Derivatives: Syntheses, Photophysical Properties and Applications," vol. 30, no. 8, p. 1659, 2025.

[10] B. A. de Marco, J. S. H. Natori, S. Fanelli, E. G. Tótoli, and H. R. N. Salgado, "Characteristics, properties and analytical methods of amoxicillin: a review with green approach," *Critical reviews in analytical chemistry,* vol. 47, no. 3, pp. 267-277, 2017.

[11] J. R. Anacona and J. Estacio, "Synthesis and antibacterial activity of cefixime metal complexes," *Transition Metal Chemistry,* vol. 31, no. 2, pp. 227-231, 2006.

[12] J. R. Anacona and I. J. J. o. C. C. Rodriguez, "Synthesis and antibacterial activity of cephalexin metal complexes," vol. 57, no. 15, pp. 1263-1269, 2004.

[13] A. Nasiri *et al.*, "Overview, consequences, and strategies for overcoming matrix effects in LC-MS analysis: a critical review," vol. 146, no. 20, pp. 6049-6063, 2021.

[14] R. Ali and M. M. J. F. C. El-Wekil, "A dual-recognition-controlled electrochemical biosensor for selective and ultrasensitive detection of acrylamide in heat-treated carbohydrate-rich food," vol. 413, p. 135666, 2023.

[15] M. Zermane *et al.*, "Modeling approach for Ti3C2 MXene-based fluorescent aptasensor for amoxicillin biosensing in water matrices," vol. 360, p. 121072, 2024.

[16] M. R. L. Stone, M. S. Butler, W. Phetsang, M. A. Cooper, and M. A. J. T. i. b. Blaskovich, "Fluorescent antibiotics: new research tools to fight antibiotic resistance," vol. 36, no. 5, pp. 523-536, 2018.

[17] A. Golcu, B. Dogan, and S. A. J. T. Ozkan, "Anodic voltammetric behavior and determination of cefixime in pharmaceutical dosage forms and biological fluids," vol. 67, no. 4, pp. 703-712, 2005.

[18] J.-C. G. J. C. r. Bünzli, "Lanthanide luminescence for biomedical analyses and imaging," vol. 110, no. 5, pp. 2729-2755, 2010.

[19] T. Behrsing, G. B. Deacon, and P. C. Junk, "The chemistry of rare earth metals, compounds, and corrosion inhibitors," in *Rare Earth-Based Corrosion Inhibitors*: Elsevier, 2014, pp. 1-37.

[20] A. Karmakar, P. Samanta, S. Dutta, and S. K. J. C. A. A. J. Ghosh, "Fluorescent “turn-on” sensing based on metal–organic frameworks (MOFs)," vol. 14, no. 24, pp. 4506-4519, 2019.

[21] S. A. Younis, N. Bhardwaj, S. K. Bhardwaj, K.-H. Kim, and A. J. C. C. R. Deep, "Rare earth metal–organic frameworks (RE-MOFs): Synthesis, properties, and biomedical applications," vol. 429, p. 213620, 2021.

[22] S. V. Eliseeva and J.-C. G. J. C. S. R. Bünzli, "Lanthanide luminescence for functional materials and bio-sciences," vol. 39, no. 1, pp. 189-227, 2010.

[23] S. Jana, R. P. Ojha, R. Shyam, R. J. S. A. P. A. M. Prakash, and B. Spectroscopy, "Isoniazid (INH) a tuberculosis drug detection using turn-off fluorescent [Ce (o-Van) 3 (H2O) 3] probe in real samples," vol. 337, p. 126057, 2025.

[24] S. Jana, R. P. Ojha, R. J. S. A. P. A. M. Prakash, and B. Spectroscopy, "A novel turn-on fluorescence sensor based on the Nd (III) complex for the ultrasensitive detection of 6-mercaptopurine," vol. 313, p. 124056, 2024.

[25] D. M. Pavlović, S. Babić, A. J. Horvat, and M. J. T. T. i. A. C. Kaštelan-Macan, "Sample preparation in analysis of pharmaceuticals," vol. 26, no. 11, pp. 1062-1075, 2007.

[26] Y. Shi, G. Naren, Y. Zhang, J. Han, A. J. O. Bohnuud, and L. Technology, "Synthesis, Structures, optical properties and DFT studies of neodymium complexes containing octanoyl amino carboxylic acids," vol. 155, p. 108445, 2022.

[27] T. M. Lovestead and K. J. A. H. Urness, UK, "Gas Chromatography-Mass Spectrometry (GC-MS)," 2019.

[28] S. Nasiri *et al.*, "Modified Scherrer equation to calculate crystal size by XRD with high accuracy, examples Fe2O3, TiO2 and V2O5," vol. 3, p. 100015, 2023.

[29] A. Khalil, A. Shaaban, M. Azab, A. Mahmoud, and A. J. J. o. P. R. Metwally, "Synthesis, characterization and morphology of polyanthranilic acid micro-and nanostructures," vol. 20, no. 6, p. 142, 2013.

[30] M. Nawaz *et al.*, "Synthesis of metal anthranilate complexes: catalytic and antipathogenic studies," vol. 16, no. 1, p. 21, 2022.

[31] C. A. Southern, D. H. Levy, G. M. Florio, A. Longarte, and T. S. J. T. J. o. P. C. A. Zwier, "Electronic and infrared spectroscopy of anthranilic acid in a supersonic jet," vol. 107, no. 20, pp. 4032-4040, 2003.

[32] J.-C. G. Bünzli and S. V. Eliseeva, "Basics of lanthanide photophysics," in *Lanthanide luminescence: photophysical, analytical and biological aspects*: Springer, 2010, pp. 1-45.

[33] M. Hasegawa, H. Ohmagari, H. Tanaka, K. J. J. o. P. Machida, and P. C. P. Reviews, "Luminescence of lanthanide complexes: From fundamental to prospective approaches related to water-and molecular-stimuli," vol. 50, p. 100484, 2022.

[34] A. Nardecchia, V. Motto-Ros, and L. J. A. C. A. Duponchel, "Saturated signals in spectroscopic imaging: why and how should we deal with this regularly observed phenomenon?," vol. 1157, p. 338389, 2021.

[35] B. J. I. C. F. Yan, "Luminescence response mode and chemical sensing mechanism for lanthanide-functionalized metal–organic framework hybrids," vol. 8, no. 1, pp. 201-233, 2021.

[36] G. Nocton, A. Nonat, C. Gateau, and M. J. H. C. A. Mazzanti, "Water Stability and Luminescence of Lanthanide Complexes of Tripodal Ligands Derived from 1, 4, 7-Triazacyclononane: Pyridinecarboxamide versus Pyridinecarboxylate Donors," vol. 92, no. 11, pp. 2257-2273, 2009.

[37] B. Monteiro *et al.*, "Lanthanide-based complexes as efficient physiological temperature sensors," vol. 277, p. 125424, 2022.

[38] D. J. A. o. C. R. Escudero, "Revising intramolecular photoinduced electron transfer (PET) from first-principles," vol. 49, no. 9, pp. 1816-1824, 2016.

[39] C. Alexander, "Exploring new paths towards biological anion recognition by lanthanide complexes," University of Oxford, 2022.

[40] J. R. Lakowicz, *Principles of fluorescence spectroscopy*. Springer, 2006.

[41] R. Otto, M. R. Ferguson, K. Marro, J. W. Grinstead, and S. D. J. P. r. Friedman, "Limitations of using logarithmic transformation and linear fitting to estimate relaxation rates in iron-loaded liver," vol. 41, no. 10, pp. 1259-1265, 2011.

[42] J. M. Ha, S. H. Hur, A. Pathak, J.-E. Jeong, and H. Y. J. N. A. M. Woo, "Recent advances in organic luminescent materials with narrowband emission," vol. 13, no. 1, p. 53, 2021.

[43] K. J. C. C. R. Binnemans, "Interpretation of europium (III) spectra," vol. 295, pp. 1-45, 2015.

[44] H. Yang, G. Ran, J. Yan, H. Zhang, and X. Hu, "A sensitive fluorescence quenching method for the detection of tartrazine with acriflavine in soft drinks," *Luminescence,* vol. 33, no. 2, pp. 349-355, 2018.

[45] V. Pandey and T. J. L. Pandey, "Spectroscopic Visualization of Drug–Biomolecules Interactions: An Insight to Fluorescence Quenching as Tool in Drug Discovery," vol. 40, no. 4, p. e70168, 2025.

[46] F. Pena-Pereira, W. Wojnowski, and M. J. A. c. Tobiszewski, "AGREE—Analytical GREEnness metric approach and software," vol. 92, no. 14, pp. 10076-10082, 2020.

[47] S. P. Pawar *et al.*, "Fluorescence-based sensor for selective and sensitive detection of amoxicillin (Amox) in aqueous medium: Application to pharmaceutical and biomedical analysis," vol. 32, no. 6, pp. 918-923, 2017.

[48] A. Muthukumar and S. J. J. o. F. Kalaiyar, "Fluorescence Entrenched Probe for Onsite Detection of Amoxicillin Residue in Bovine Milk," pp. 1-12, 2024.

[49] X. Zhang, Y. Ren, Z. Ji, and J. J. J. o. M. L. Fan, "Sensitive detection of amoxicillin in aqueous solution with novel fluorescent probes containing boron-doped carbon quantum dots," vol. 311, p. 113278, 2020.

[50] K. F. Azeez, A. Salimi, H. J. S. Mohtasham, and A. Reports, "Ratiometric fluorescence quantitation of amoxicillin based on CDs@ Eu-MOFs incorporated 3D hydrogel using smartphone-assisted portable dual mode visual sensing," vol. 9, p. 100262, 2025.

[51] F. Akhgari, N. Samadi, and K. J. J. o. f. Farhadi, "Fluorescent carbon dot as nanosensor for sensitive and selective detection of cefixime based on inner filter effect," vol. 27, no. 3, pp. 921-927, 2017.

[52] N. Bukhari, A. A. Al-Warthan, S. M. Wabaidur, Z. A. Othman, M. Javid, and S. J. S. L. Haider, "Spectrofluorimetric determination of cefixime in pharmaceutical preparation and biological fluids using calcein as a fluorescence probe," vol. 8, no. 2, pp. 280-284, 2010.

[53] J. Shah, M. R. Jan, S. Shah, and I. J. J. o. fluorescence, "Spectrofluorimetric method for determination and validation of cefixime in pharmaceutical preparations through derivatization with 2-cyanoacetamide," vol. 21, no. 2, pp. 579-585, 2011.

[54] J. L. Manzoori, M. Amjadi, N. Soltani, and A. J. I. j. o. b. m. s. Jouyban, "Spectrofluorimetric determination of cefixime using terbium-danofloxacin probe," vol. 17, no. 4, p. 256, 2014.

[55] A.-Y. Hao *et al.*, "A smartphone-combined ratiometric fluorescence probe for specifically and visibly detecting cephalexin," vol. 249, p. 119310, 2021.

[56] L. Li, Q. Zhang, Y. Ding, X. Cai, S. Gu, and Z. J. A. M. Cao, "Application of l-cysteine capped core–shell CdTe/ZnS nanoparticles as a fluorescence probe for cephalexin," vol. 6, no. 8, pp. 2715-2721, 2014.

[57] S. Sahu, M. Karuppusamy, S. J. B. Easwaramoorthi, and B. X, "Water-dispersible polymer coated silica nanoparticle for turn-on fluorometric detection of Cephalexin," vol. 12, p. 100231, 2022.